Solar Energy Materials & Solar Cells ▮ (▮▮▮▮) ▮▮▮–▮▮▮

Contents lists available at ScienceDirect

Solar Energy Materials & Solar Cells

journal homepage: www.elsevier.com/locate/solmat

Thin film silicon n–i–p solar cells deposited by VHF PECVD at 100 °C substrate temperature

M. Brinza, J.K. Rath *, R.E.I. Schropp

Faculty of Science, Department of Physics and Astronomy, SID-Physics of Devices, Utrecht University, P.O. Box 80000, 3508 TA Utrecht, The Netherlands

ARTICLE INFO

Article history:
Received 14 January 2008
Accepted 16 September 2008

Keywords:
Silicon
Microcrystalline
Amorphous
PECVD
Thin film
Solar cell
Low temperature

ABSTRACT

The applicability of the very high frequency (VHF) plasma-enhanced chemical vapor deposition (PECVD) technique to the fabrication of solar cells in an n–i–p configuration at 100 °C substrate temperature is being investigated. Amorphous and microcrystalline silicon cells are made with the absorber layers grown in conditions close to the amorphous-to-microcrystalline transition, which proved to give the best quality layers. It was observed that post-deposition annealing at 100 °C resulted in a relative increase of the efficiency of up to 50% for both amorphous and microcrystalline cells. For an amorphous solar cell deposited on stainless steel foil with a non-textured back reflector, an efficiency of 5.3% was achieved. A too rough substrate (textured back reflector), with an rms roughness higher than 80 nm, was found to give rise to shunting paths.

1. Introduction

In the last couple of years, research on deposition of thin film silicon layers at a very low substrate temperature (around 100 °C and below) for photovoltaic applications has received considerable attention. This process temperature opens the way for a variety of unconventional temperature-sensitive polymer substrates, such as polyethylene terephthalate (PET), polyethylene (PE) or polycarbonate (PC) for thin film silicon device applications. The plastic substrates have the advantages of being cheap, light and flexible. However, material optimization has to be achieved first, especially in two aspects, microscopic and macroscopic defects.

(1) Decreasing the substrate temperature below the standard optimum temperature of 200–250 °C results in a pronounced deterioration of the optoelectronic properties of Si thin films [1]. This is attributed to an increase of microscopic defects such as dangling bond defects and weak bonds, which not only can lead to lower initial efficiency of solar cells but also to more light-induced degradation. Optimizing hydrogen dilution can provide a solution to both of these problems. At standard substrate temperatures, the admixing of hydrogen into the feedstock gas silane (hydrogen dilution) was shown to be beneficial to the stability of solar cells against light-induced degradation [2 and references therein], due to an increased medium-range order of the amorphous network [3,4]. Such a material, deposited in the proximity of the amorphous-to-microcrystalline transition but on the amorphous side, is often called "protocrystalline" silicon. Likewise, hydrogen dilution offers the key to improve the material quality at low deposition temperature [5].

(2) Low temperature induces macroscopic defects such as elongated void structure and columnar amorphous growth [6]. However, the effect of the substrate on such defects has not been studied to a large extent. It has been observed for depositions at standard temperatures (~200 °C) that the amount of defects in the silicon layer increases with the increase in substrate roughness [7] leading to shunting. In this paper, we intend to find the influence of surface roughness on the characteristics of solar cells deposited at low substrate temperature. This will lead to optimization of back reflector (BR) specifically for low-temperature deposition. Moreover, from a material point of view, puzzling properties of Si films grown at a very low temperature are often observed. In Ref. [8] it is reported that for materials deposited at 60 °C and below, Raman spectroscopy shows the 520 cm^{-1} peak associated with the TO mode in crystalline structure, while X-ray diffraction, carrier transport and optical properties have an amorphous-like behavior. A thorough characterization of the materials at the transition regime is thus essential.

Reported conversion efficiencies for solar cells deposited at around 100 °C substrate temperature using plasma-enhanced

* Corresponding author. Tel.: +31 302532345.
E-mail address: j.k.rath@phys.uu.nl (J.K. Rath).

0927-0248/$ - see front matter © 2008 Elsevier B.V. All rights reserved.
doi:10.1016/j.solmat.2008.09.013

chemical vapor deposition (PECVD) at a standard frequency of 13.56 MHz or in the very high frequency (VHF) regime (50–80 MHz) are in the range of 5–7% under AM1.5 illumination. Ishikawa et al. [9] obtained 5.6% initial efficiency for an n–i–p cell deposited at 110 °C on an opaque substrate coated with an Al/ZnO:Al BR. The cells in the n–i–p configuration had better stability against light-induced degradation in comparison with the p–i–n structure with an identical i-layer. Previous work performed in our group showed that a-Si:H layers deposited at 100 °C by VHF PECVD could successfully be used in p–i–n solar cells on a glass/TCO superstrate which yielded 7.3% efficiency under AM1.5 illumination [10]. The integration of similar intrinsic material in the n–i–p configuration is now being investigated. We also show initial results on microcrystalline silicon n–i–p cells. The intended applications include tandem cells deposited on temperature-sensitive (opaque) substrates like plastics and paper.

2. Experimental

For the present study, a series of n–i–p solar cells was deposited on stainless steel (SS) foil substrates by VHF PECVD at 50 MHz in our ultra-high vacuum multichamber system ASTER, in which the hydrogen dilution ratio $R_H = [H_2]/[SiH_4]$ of the process gas for the deposition of the intrinsic silicon layers was varied between 5 and 25, such that the amorphous-to-microcrystalline threshold was crossed within this series. The substrate temperature was kept at 100 °C. For some of the samples the SS substrate was coated with an Ag/ZnO double layer deposited by RF magnetron sputtering to act as a (textured) BR. ITO top contacts with Au grid lines define the cells with an active area of 0.13 cm^2. For the study of individual layers HF-dipped Corning 2000 glass was used as a substrate while evaporated Ag coplanar contacts with a gap of 0.5 mm were used for electrical measurements. The photoresponse (σ_{ph}/σ_d) of the samples is defined as the ratio of the AM1.5 photoconductivity and the dark conductivity. The subbandgap absorption $\alpha(h\upsilon)$ was measured using the constant photocurrent method (CPM) and photothermal deflection spectroscopy (PDS). The crystallinity of the layers was evaluated using the Raman spectroscopy. The Raman crystalline ratio is defined as $R_c = (I_{510}+I_{520})/(I_{480}+I_{510}+I_{520})$, where I_{480}, I_{510}, and I_{520} are the intensities of the transverse optic (TO) mode in a-Si, grain boundaries and/or small grains, and c-Si, respectively. Raman spectra were recorded using the 514.5 nm line of an Ar^+ laser, a triple-grating monochromator and a CCD camera. The solar cell efficiency was measured with a dual-beam solar simulator (Wacom, Japan) under 100 mW/cm^2 AM1.5 illumination. Surface imaging was performed with an atomic force microscope (AFM) in tapping mode and the AFM images were analyzed using the WSxM software [11].

3. Results and discussion

3.1. Individual layer characterization

The solar cell efficiency is directly influenced by the electronic quality of the intrinsic layer. For this reason, it is essential to identify the optimum deposition regime of amorphous and microcrystalline layers, which is scanned for the present series of samples by varying the hydrogen dilution ratio. Fig. 1 shows the Raman crystalline ratio, the activation energy, the Urbach energy of the amorphous samples and the photoresponse throughout the dilution series. In agreement with common knowledge, the best amorphous and microcrystalline materials at 100 °C are grown in the vicinity of the amorphous-to-microcrystalline transition

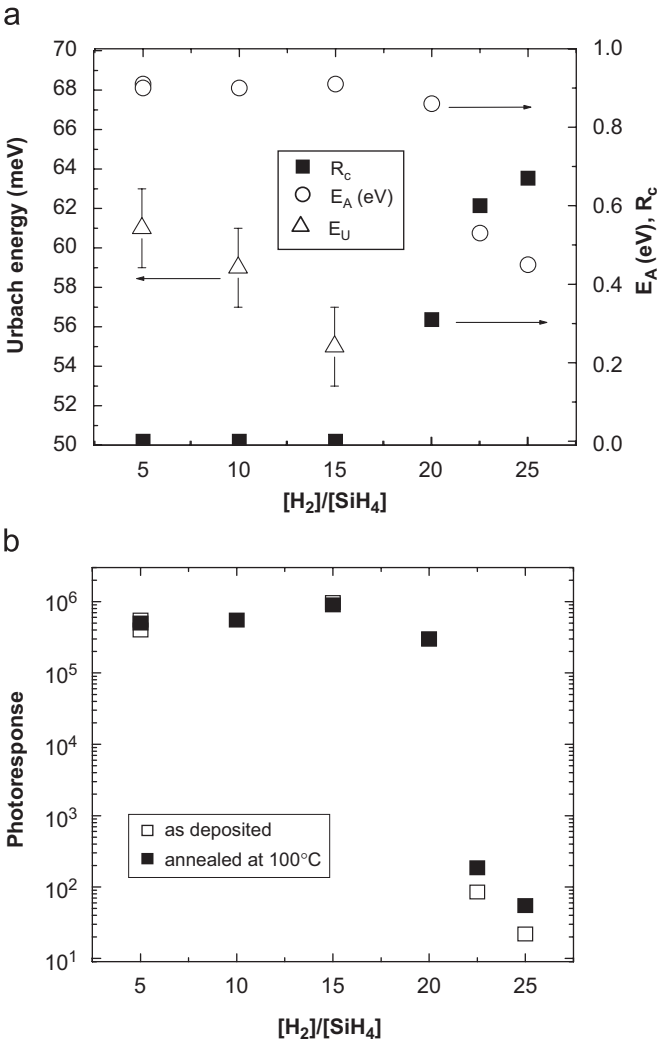

Fig. 1. (a) Raman crystalline ratio (R_c), activation energy (E_A) and Urbach energy (E_U) of the amorphous layers and (b) photoresponse versus hydrogen dilution ratio $[H_2]/[SiH_4]$.

which takes place at $R_H > 15$. The a-Si:H layer deposited just before the transition ($R_H = 15$) has an Urbach energy as low as 55 meV and a midgap defect density of 2×10^{16} cm^{-3}, as evaluated from the CPM absorption coefficient at 1.2 eV, using a proportionality factor of 2×10^{16}. The photoresponse of the amorphous layer is 9×10^5 while the μc-Si:H material deposited close to the threshold ($R_H = 22.5$) has a photoresponse of 80 as deposited. The photoresponse increased to 180 after annealing at 100 °C for 2 h.

A microcrystalline p-type layer was chosen as a window layer for the cells, due to its high optical bandgap and good electrical properties. It is known that the nucleation of crystallites in the boron-doped silicon layer depends on the type of the substrate [12]. For this reason and for characterization purposes, the p-layer was grown on top of a stack consisting of a 20 nm a-Si:H layer (deposited on glass) and a buffer layer of about 2 nm thickness. The role of the buffer layer (a material that is deliberately low-quality, grown at $R_H = 1$ and 100 °C) in the solar cell structure is on the one hand to facilitate the nucleation of the p-type doped layer and on the other hand to suppress electron back diffusion caused by the band offset at the conduction band edge between the amorphous i-layer and the microcrystalline p-layer. The best p-type layer, which was subsequently used in solar cells, has a Raman crystalline ratio of 0.29, an activation energy of 0.19 eV, a dark conductivity of 4×10^{-3} Ω^{-1} cm^{-1} and a thickness of 34 nm.

Please cite this article as: M. Brinza, et al., Sol. Energy Mater. Sol. Cells (2008), doi:10.1016/j.solmat.2008.09.013

3.2. Transition regime

The intrinsic layer deposited at $R_H = 20$ deserves special discussion. As can be seen in Fig. 1, it shows a Raman crystalline fraction of 0.31 but the activation energy and the photoresponse have values typical for a-Si:H. Fig. 2 shows an AFM scan of a $10 \times 10\,\mu m^2$ region of this sample. According to the knowledge gained in this field [6,13], the protruding features correspond to microcrystalline grains sticking out from the amorphous background. The electrical measurements can be explained by the lack of a percolation path between the microcrystallites in the lateral direction, in which case the current is flowing through the amorphous tissue. CPM measurements, in which a photocurrent is recorded and kept constant, give an amorphous-like absorption coefficient spectrum, with an Urbach edge of 62 ± 3 meV, while PDS, which is a contactless method, shows an increased absorption at 1.4 eV, indicating the presence of the microcrystalline fraction.

In a cell, the same material behaves as microcrystalline ($V_{OC} = 0.4$ eV). One can assume that the microcrystalline grains ensure electrical conduction in the vertical direction. Besides, it can be speculated that the underlying *n*-layer (with a Raman crystalline ratio of 0.76) promotes crystallinity in the intrinsic layer. The crystalline ratio measured from the top of the cell is 0.44, but it is not possible to distinguish the contributions of the p-type doped layer and the intrinsic layer.

3.3. The effect of the substrate texture

The textured BR, mostly used for solar cells in a substrate configuration (n–i–p), consists of a stack of sputtered Ag and ZnO:Al layers. The degree of the substrate texture is linked to the size of the grains of the polycrystalline Ag films, which is in turn controlled by the substrate temperature during the deposition of the Ag layers and the thickness of the Ag layer itself [14]. Although the fabrication method of such BR is, generally speaking, not compatible with temperature-sensitive plastic substrates, test BRs were sputter-deposited at a substrate temperature ranging from about 110 °C (for "cold" substrate where the heating is solely due to the plasma energetic ion bombardment) to about 300 °C in order to investigate how much the substrate texture can enhance the short-circuit current in the cells. Preliminary studies on n–i–p cells, deposited at $R_H = 5$, on several differently textured substrates, showed that an rms roughness σ of 80 nm and higher causes all cells of the sample to be shunted. For cells deposited on smoother substrates this problem was not encountered. The rms roughness and the lateral size of the Ag grains, estimated from $5 \times 5\,\mu m^2$ AFM scans of Ag+ZnO layers on SS, are shown in Table 1, together with the relative improvement of the short-circuit current.

Considering the growth of the Si films on a rough substrate surface and taking into account the low surface diffusion of the deposited species associated with the low substrate temperature, the formation of (elongated) voids in the Si films is expected. When such a void structure is filled with ITO from the top contact, it creates a shunting path. Such voids were reported to appear in hot-wire μc-Si:H deposited at 250 °C at the position of acute angles between Ag grains [7]. Diffusion of boron impurities from the p-layer through this void structure also cannot be ruled out.

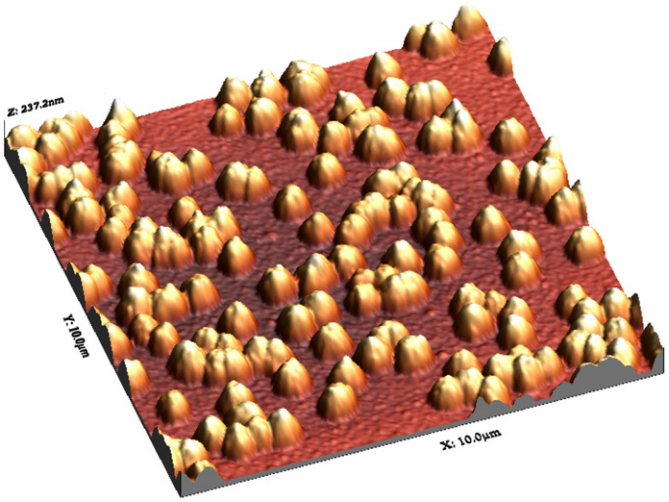

Fig. 2. AFM scan of a-Si layer deposited at 100 °C and a dilution ratio of $R_H = 20$ on glass.

3.4. Amorphous and microcrystalline solar cells

The intrinsic amorphous layer deposited at $R_H = 15$ was incorporated in two solar cell samples, with a thickness of the absorber layer of 470 nm. For the first sample, the best cell of which is reported in Table 2, both the p- and n-doped layers were chosen microcrystalline and plain SS was used as a substrate. The efficiency of initially 3.0% improves significantly upon post-deposition annealing at 100 °C for about 2 h, reaching 4.2%. However, the V_{oc} value after annealing remains quite small for a large bandgap material (with a Tauc gap of 1.9 eV). Since the nature of the substrate can affect the structure of the film grown on top of it, especially when the growth occurs close to the microcrystalline threshold, the second sample is deposited with a double n-layer consisting of a microcrystalline bottom part and an amorphous top part. The best cells of this sample deposited on plain SS and SS/"cold" Ag/ZnO are reported in Table 3. The obvious improvement with the use of a double n-layer is the increase of open circuit voltage when the i-layer is deposited on an amorphous n-layer. Fig. 3 shows the light *J–V* characteristics of all studied cells. Note that, even if the BR is only slightly textured

Table 1
Characteristic parameters of back reflectors with different textures, where T is the substrate temperature, d is the thickness of the Ag layer, σ is the rms roughness and L is the lateral feature size

T (°C) ± 50 °C	d (nm) ± 50 nm	σ (nm) ± 5 nm	L (nm) ± 50 nm	δJ_{sc} (%)
300	750	> 150	> 1500	–
200	750	80	1000	–
150	650	60	800	42
100	500	35	550	29
100	270	20	550	14

δJ_{sc} is the relative improvement of the short-circuit current of cells deposited on the respective back reflectors ("–" denotes shunted cells) with respect to J_{sc} of cells deposited on plain SS.

Table 2
AM1.5 output parameters of an a-Si:H solar cell on plain SS with microcrystalline-doped layers

State	Eff. (%)	J_{sc} (mA/cm^2)	V_{oc} (V)	FF
AD	3.0	9.0	0.66	0.50
ANN	4.2	10.0	0.72	0.58

State AD means as deposited and ANN refers to the state after annealing at 100 °C for roughly 2 h. The *J–V* characteristics were recorded without a mask.

Please cite this article as: M. Brinza, et al., Sol. Energy Mater. Sol. Cells (2008), doi:10.1016/j.solmat.2008.09.013

Table 3
AM1.5 output parameters of an a-Si:H solar cell on (a) plain SS and (b) Ag/ZnO coated SS with double n-doped layer and microcrystalline p-doped layer

State	Eff. (%)	J_{sc} (mA/cm^2)	V_{oc} (V)	FF
(a) AD	3.9	9.0	0.77	0.55
(a) ANN	4.7	9.6	0.84	0.57
(b) AD	4.8	10.7	0.82	0.55
(b) ANN	5.3	11.2	0.84	0.52

The *J–V* characteristics were recorded without a mask.

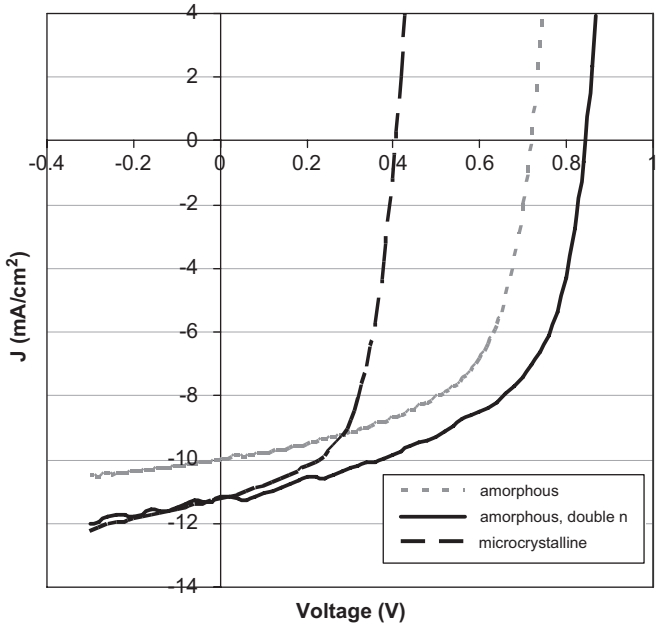

Fig. 3. *J–V* characteristics for the cells listed in Table 2 (amorphous), Table 3 (amorphous, on a double n-layer) and Table 4 (microcrystalline).

Table 4
AM1.5 output parameters of a μc-Si:H solar cell on plain SS

State	Eff. (%)	J_{sc} (mA/cm^2)	V_{oc} (V)	FF
AD	1.7	9.6	0.32	0.55
ANN	2.6	11.3	0.41	0.58

The *J–V* characteristics were recorded without a mask.

(rms roughness = 20 nm, see Table 1), it already gives an improvement in the short-circuit current. From spectral response measurements, an improvement of the carrier collection in the red part of the spectrum could indeed be seen. In order to avoid the lateral collection, the *J–V* characteristics can be measured with a mask. The efficiencies in this case are somewhat lower; for example, for the cell reported in Table 2 in the annealed state, 3.9% is obtained for the cell on substrate (a) and 4.5% for the cell on substrate (b). On the other hand, the use of a mask can underestimate photocurrents due to shadowing effects.

Table 4 reports the best cell of a microcrystalline sample deposited on plain SS at $R_H = 22.5$ dilution for the 1 μm thick intrinsic layer. As was also observed in the amorphous case, this cell benefits from post-deposition annealing at 100 °C.

3.5. Annealing effects

The observed improvement in the solar cell efficiency upon annealing is in most cases due to an increase in the open circuit voltage, which can be attributed to a decrease in the activation energy of the p-layer upon annealing as well as to an improvement of the p/ITO interface. Furthermore, an increase of the conductivity of the p-layer, which also affects the quality of the p/ITO junction, can explain the small increase in the short-circuit current. A study of the individual p-doped layer deposited on Corning 2000 glass confirmed that its conductivity increases and its activation energy decreases upon repeated annealing cycles at 100 °C. On the other hand, we cannot rule out an improvement of the intrinsic layers in the solar cells with annealing. An increase of the photoresponse of the microcrystalline layers was actually observed, as already mentioned.

4. Conclusions

The use of a double n-layer (the first being microcrystalline, the second amorphous) instead of a single microcrystalline layer improves the V_{oc} (from 0.72 to 0.84 V) of amorphous silicon cells deposited at 100 °C with the absorber layer grown close to the transition threshold. Post-deposition annealing at 100 °C for about two hours has a positive effect on both the V_{oc} and J_{sc} and thus on the solar cell efficiency. At the low fabrication temperatures used here, there is a higher probability of shunting of cells when grown on rough substrates. The highest efficiency achieved in an all-100 °C cell amorphous silicon deposited on SS coated with a non-textured BR was 5.3%.

Acknowledgements

This research was financially supported by the Netherlands Agency for Energy and the Environment (SenterNovem) of the Ministry of Economic Affairs: regeling 'Energie Onderzoek Subsidie: lange termijn' (EOS LT). We thank Caspar van Bommel for the deposition of the samples.

References

[1] A. Matsuda, Jpn. J. Appl. Phys. 43 (2004) 7909.
[2] R.J. Koval, J. Koh, Z. Lu, L. Jiao, R.W. Collins, C.R. Wronski, Appl. Phys. Lett. 75 (1999) 1553.
[3] D.V. Tsu, B.S. Chao, S.R. Ovshinsky, S. Guha, J. Yang, Appl. Phys. Lett. 71 (1997) 1317.
[4] S. Guha, J. Yang, D.L. Williamson, Y. Lubianiker, J.D. Cohen, A.H. Mahan, Appl. Phys. Lett. 74 (1999) 1860.
[5] C. Koch, M. Ito, M. Schubert, Sol. Energy Mater. Sol. Cells 68 (2001) 227.
[6] P.C.P. Bronsveld, J.K. Rath, R.E.I. Schropp, T. Mates, A. Fejfar, B. Rezek, J. Kocka, Appl. Phys. Lett. 89 (2006) 051922.
[7] H. Li, R. Franken, R.L. Stolk, J.K. Rath, R.E.I. Schropp, Solid State Phenom. 131–133 (2008) 27.
[8] M. Ito, K. Ro, S. Yoneyama, Y. Ito, H. Uyama, T. Mates, M. Ledinsky, K. Luterova, P. Fojtik, H. Stuchlikova, A. Fejfar, J. Kocka, Thin Solid Films 442 (2003) 163.
[9] Y. Ishikawa, M.B. Schubert, in: Proceedings of the 20th EUPVSEC, Barcelona, 2005, p. 1525.
[10] P.C.P. Bronsveld, J.K. Rath, R.E.I. Schropp, Proceedings of the 20th EUPVSEC, Barcelona, 2005, p. 1675.
[11] I. Horcas, R. Fernández, J.M. Gómez-Rodríguez, J. Colchero, J. Gómez-Herrero, A.M. Baro, Rev. Sci. Instrum. 78 (2007) 013705.
[12] J.K. Rath, R.E.I. Schropp, Sol. Energy Mater. Sol. Cell 53 (1998) 189.
[13] T. Mates, P.C.P. Bronsveld, A. Fejfar, B. Rezek, J. Kocka, J.K. Rath, R.E.I. Schropp, J. Non-Cryst. Solids 352 (2006) 1011.
[14] R.H. Franken, R.L. Stolk, H. Li, C.H.M. van der Werf, J.K. Rath, R.E.I. Schropp, J. Appl. Phys. 102 (2007) 014503.